A Comparison of Plastic Collapse and Limit Loads for Single Mitred Pipe Bends Under In-Plane Bending.

R. Neilson[b], J. Wood[a], R. Hamilton[b] and H. Li[b].

[a] Department of Mechanical Engineering, University of Strathclyde, 75 Montrose Street, Glasgow G1 1XJ, UK (corresponding author).

[b] Department of Mechanical Engineering, University of Strathclyde, 75 Montrose Street, Glasgow G1 1XJ, UK

Abstract

This paper presents a comparison of the plastic collapse loads from experimental in-plane bending tests on three 90 degree single un-reinforced mitred pipe bends, with the results from various 3D solid finite element models. The bending load applied reduced the bend angle and in turn, the resulting cross-sectional ovalisation led to a recognised weakening mechanism, which is only observable by testing or by including large displacement effects in the plastic finite element solution. A small displacement limit solution with an elastic-perfectly-plastic material model overestimated the collapse load by 40%. The plastic collapse finite element solution produced excellent agreement with experiment.

Keywords: Mitred pipe bend; plastic collapse, limit, experimental, finite element analysis.

1. Introduction

Mitred joints are widely used in modern building structures such as shopping centres, as well as an alternative to smooth bends in the more traditional areas such as chemical complexes, de-salination plants, water supply and nuclear power stations. Mitred bends are also finding application in new designs of fusion and pebble-bed reactors. In some cases, they are used where the manufacture of smooth bends may be either impractical due to restricted space or uneconomical. Many of these applications are low duty and most piping and pressure vessel codes will limit application. However, there is still a need to know the margins of safety when using such a design detail. In addition, knowing the significance of any weakening or strengthening mechanisms in relation to the collapse load is also important. Figure 1 introduces some of the terminology associated with mitred bends.

Figure 1: Mitre Terminology

Much of the early theoretical work on mitred bends, which related to the development and subsequent refinement of fundamental theoretical details, was often informed by comparisons with experiments. For example, early theories assumed the un-reinforced segment of a multi-mitre to have a uniform flattening and the intersection of a reinforced mitre to be rigidly constrained. Later theories relaxed these constraints and involved series expansions to allow for the decay of cross-sectional ovalisation, postulating the existence of long and short decay lengths. Such developments improved comparison with experiment. It is also apparent from the early documents that the development of the theory had much in common with smooth pipe bends. This is not surprising given that the basic behaviour of these components is similar. This includes the fact that both develop an increase in flexibility and local stress levels due to cross-

section ovalisation. The mitre obviously has the added complexity of discontinuity stresses at the intersection. In the early theoretical work, an edge solution was developed for this case, which was then superimposed on the flattening analysis.

The later papers invariably contain the refined theories and provide best comparisons with experiment in general. Theoretical solutions for mitred bends were invariably elastic and would not be applicable to the present investigation.

Today, the Finite Element Method has a dominant role in the study of engineering structures and components in general and most organisations faced with the need to examine a mitred pipe bend will almost certainly use this as the preferred approach.

The use of Design by Analysis and Finite Element Analysis in particular is increasing [1]. In addition, models are becoming larger and more detailed. Analysis types are also becoming more complex. The issue of validating such models against quality physical experiments is increasing in importance as analytical solutions become less relevant. It is also widely recognised that benchmarking finite element results against quality experimental data is a valuable exercise in terms of the education of the analyst. Comparisons with experiment also allow a study of the significance of real-world variables relating to geometry, material and boundary conditions and can be an enlightening experience for analysts. This paper provides a worthwhile addition to the literature available in this field.

2. Review of Literature on the Plastic Behaviour of Mitres Under In-Plane Bending

Wood [2] presents an up-to-date and comprehensive list of almost all references relating to the structural behaviour of mitred pipe bends of all types. The post-yield information available in the literature relates to either limit/burst pressure tests or limit/collapse bending moment tests - either in-plane or out-of-plane. Only the bending moment literature will be discussed in this

paper. In addition, the nonlinear effects of combined pressure and bending will not be covered in detail.

So[3] carried out a successful in-plane bending collapse test for a 90^0 single un-reinforced mitre pipe bend, manufactured from aluminium. Although not specifically mentioned, it would appear that the in-plane bending moment was tending to close the bend i.e. reduce the bend angle. A collapse load 'F_L' of 6161N was reported for this test. This compared to a 'gross yield' load 'F_{GY}' of 1868N and a 'first yield' load 'F_{FY}' of 1339N, giving an F_L/F_{GY} ratio of 3.3 and a first yield ratio F_L/F_{FY} of 4.6. It was noted in this experiment that the load/deflection behaviour of the bend became time dependent at loads above 2002N. The test on a 120^0 bend was ended prematurely, due to a failure in the test arrangement.

Kitching, Rahimi & So[4] compared shell finite element results with the experimental results for the post-yield behaviour of the two aluminium bends with unequal leg lengths, reported by So[3]. The difference between the finite element and experimental results is appreciable and this was thought to be partly due to the fact that the finite element model assumed an elastic-perfectly plastic material model, whereas the real bend material showed significant strain hardening. In his PhD thesis, Rahimi[5] presents results for 3 stainless steel mitres, with different bend angles, under in-plane bending. The ratios of collapse moment 'M_L' to general yield moment 'M_{GY}' were 2.7, 2.2 and 1.9 for the specimens with 90^0, 120^0 and 150^0 bend angles respectively. Rahimi reported favourable comparison with large displacement finite element models.

A parametric survey for the in-plane limit moment of single mitres was presented by Robinson & Babaii Kockekseraii[6]. The 'upper bound' results were obtained using shell finite element models. The same parametric results were also presented by Babaii Kockekseraii[8], along with a comparison against the experimental results of [4]. The importance of including large displacement effects in the analysis of bends with combined pressure and bending loads was

highlighted by Babaii Kockekseraii [7] and the dependence of the final stress state on loading sequence was also illustrated.

In 2002, Gresnigt[9] presented elastic and plastic results for various single mitres when subjected to in-plane bending, with and without a fixed internal pressure. Although collapse loads and deformations are not discussed, the author presents both elastic and plastic 'limit' values. For the deformations, these limit values are in general much smaller than those at the end of the test. The ratio of plastic to elastic 'deformation capacity' varies between 4.7 and 6.8 over the range of tests. In this case, the ratios relate to the angular rotation of the bend at a set distance from the mitre intersection, taken from the load-deflection plots at departure from linearity (elastic) and at maximum load (plastic). The cyclic load-deflection graphs clearly show ratchetting, although no comment is made on this behaviour or on the purpose of the cycling. It is also noted that the 'deformation capacity' of the mitres in bending, is considerably greater that that for a straight pipe.

Gross[10] reported that a load of 6676N was required for gross yielding of a 90^0, 5 segment, mitre (indicated by a departure from linearity of the load/deflection graph). Unfortunately, Gross did not carry the above test to failure and therefore collapse loads could not be obtained.

Lane[11] reported results from tests to failure on 90^0 double-segment specimens. For an in-plane bending moment reducing the bend angle, the first yield moment, indicated by strain gauges, 'M_{FY}' was 41759Nm, whereas the collapse moment 'M_L' was 194271Nm giving an M_L/M_{FY} ratio of 2.5. For an in-plane bending moment increasing the bend angle, the first yield moment 'M_{FY}' was 40241Nm. However, in this case, no failure was indicated at 264475Nm and the test was discontinued. This indicated an M_L/M_{FY} ratio> 6.5.

Lane[12] reported results from tests to failure on 90^0 single segment mitres. For an in-plane bending moment reducing the bend angle, the general yield moment 'M_{GY}' indicated by non-linearity of load/deflection plot, was 47833Nm, whereas the collapse moment 'M_L' was

95160Nm, giving an M_L/M_{GY} ratio of 2.0. For an in-plane bending moment increasing the bend angle, the general yield moment 'M_{GY}' was approximately 97691Nm. Unfortunately, during this test the rig failed, therefore precluding the determination of a collapse load. At the point of rig failure, the maximum moment applied was approximately 187284Nm, therefore the M_L/M_{GY} ratio was in excess of 1.9. The above results were also reported by Lane & Rose[13].

Bond[14] tested a 90^0, 2-segment, mitre under the action of an in-plane bending load, tending to reduce the angle of the bend, until it collapsed. The salient points from the test were that deviation from linearity of end deflection v load plot occurred at 2135N ('F_{GY}') and collapse occurred at a total end load of 4239N ('F_L') giving $F_L/F_{GY} = 2$.

Hose[15] reported the failure of five nominally identical multi-mitre piped bends, with a PVC lined GRP construction. The failure mechanisms and appearances are discussed for various loadings, including in-plane bending.

Most piping codes will attempt to ensure that the minimum thickness of the bend is such that it will guard against gross plastic deformation and will shakedown to elastic action within the first few cycles. Murali, Munshi & Kushwaha[16] discussed the possible extension of the 'B' index for mitred bends in ASME III Boiler and Pressure Vessel Code NB3600[17], to radius to thickness ratios 'a/t' > 25. The authors utilised finite element models with both geometric and material nonlinearity to examine the plastic buckling and collapse of a range of 2-segment mitres, with varying a/t ratio, under in-plane bending.

It is apparent from this review of literature that limit and collapse loads are not yet available across the entire spectrum of mitred bends. Interestingly, all nonlinear finite element analysis of mitres to date has utilized shell elements. The results of comparisons between experiment and FEA have produced various levels of agreement.

3. Experimental Investigation

3.1 Mitre Bend Specifications

The mitred pipe bends were manufactured from cold finished seamless steel tubes with a tolerance on thickness of ±10% with a minimum of ±0.1mm and a tolerance of ±0.30mm on diameter **[18]**. The nominal dimensions of the pipe are 100mm dia. x 4mm thick. A thickness survey was carried out on sections of pipe that the bends were manufactured from. It was found that the average thickness was 4.01mm with a variation of ±4.2%. The diameter variation was also measured and found to be ±0.26mm. All dimensions are therefore within the specified tolerances.

A total of six tensile specimens were manufactured from the pipe and tested in accordance with reference **[19]**. The average values of Young's Modulus and Poisson's Ratio were obtained as 205.7GPa and 0.27 respectively. The material Yield Stress was measured as 496MPa at 2410 micro-strain and the Ultimate Stress was 280MPa at 5316 micro-strain. The failure strain was determined as approximately 20%.

Three bend specimens were arbitrarily selected from a total of seven that had been manufactured for a collapse and shakedown experimental programme. These specimens were heat treated after manufacture in an attempt to reduce residual stresses. After heat-treatment, the specimens were measured in a coordinate measurement machine. The resulting dimensions for the specimens used in the collapse tests are shown in Figure 2.

Figure 2: Mitre Specimen Details

3.2 Test Set-up and Procedure

The experimental configuration used for the collapse tests can be seen in Figure 3. The test machine used a servo-controlled hydraulic ram to apply the load and/or displacement to the bottom of the mitred pipe bends. One specimen was tested under load control and the other two under displacement control. At the top the mitre was pinned in position and the load cell inside the test machine was used to measure the applied load.

Figure 3: Test Arrangement and Instrumentation

This test configuration, while convenient, subjects the mitre intersection to a combination of bending and shear. In addition, the bending moment arm increases during the test. A linear displacement voltage transducer (LDVT) was used to measure the changing moment arm, while a digital inclinometer measured the end rotation of the specimen. Two strain gauges were used to check that the mitre was not subjected to torsion. A strain gauge pair, with individual gauge lengths of 1.6mm aligned normal and tangential to the mitre, allowed the principal strains to be monitored during the tests. A pair was also installed at the location of maximum stress, predicted by elastic FEA. The strain gauges were connected in a quarter bridge configuration and all data was logged in Labview to the same time-base.

The test procedures under displacement and load control were very similar:

1. The slack in the test rig was taken up, until the load cell started reading a load.
2. Under displacement control, the test machine was set at a speed of one millimetre per minute, as this was the same speed at which the tensile test specimens were tested. For the load control the machine applied a load at 1 kN per minute.

3. The actions were applied to the specimens up to the maximum stroke available in the test machine (approximately 100mm). This was well beyond the maximum load level sustained by the specimens.
4. The test data logged in Labview were then transferred to Excel for analysis.

4. Finite Element Analysis

4.1 Preliminary Studies

To ensure that the mesh and finite element procedures used for analysing the mitres was suitable, a study was first carried out to determine the limit load for a straight pipe of the same dimensions, subjected to pure bending. This problem is useful in that it has a closed-form solution. During this study, the number of elements was varied along the length, around the circumference and through thickness. The results showed a less than 1% error for the limit load. Unlike the mitre bend, the straight pipe however does not ovalise during deformation. While not ideal, the straight pipe does however provide some validation, as well as a useful reference base.

Using the mesh found from the straight pipe limit study as a starting point the mesh for the mitre, which exhibits more complex behaviour, was further refined. The final mesh chosen for comparative purposes had 16 elements round the circumference of the mitre, 24 along the length and 4 through the thickness.

4.2 Finite Element Model

The model was created using the nominal sizes of the mitre specimens, as shown in Figure 2. Due to symmetry of geometry, material and loading, a quarter model was constructed as shown in Figure 4. In addition to the symmetrical boundary conditions, a single node was prevented from moving in the vertical direction to prevent rigid body translation.

Figure 4: Finite Element and Material Models

The model was created using SOLID95 20-noded brick elements with 14 point integration, as implemented in the ANSYS finite element system [20]. As well as having a higher order shape function, this element also allows for a more accurate representation of the curved profile in particular and geometry in general. All previous finite element analyses of mitred bends, reported in the literature, have used shell elements. Such an approach would also have been possible in this case. This would have involved more approximations in the model however. As well as allowing a more faithful representation of geometry, a solid representation avoids the uncertainties associated with mid-surface representation of geometry (particularly at intersections) as well as the specific assumptions associated with shell theory. A solid representation introduces a singularity in stress at the intersection due to the lack of fillet radius however. While this leads to theoretically infinite elastic stresses, it has little or no effect on a collapse or limit solution. It is also observed that as available computing power steadily increases, there is a growing trend to use 3D solid representations in analyses in general.
To ensure that converged results of suitable accuracy were obtained a variety of convergence studies were carried out using these elements. The final mesh used had 16 elements around the circumference of the mitre pipe, 24 along the length and 4 through the thickness. Figure 5 shows the maximum load sustained for the variation in number of elements through the thickness. In this case, the number of elements in the circumferential direction was fixed at 16. It may be observed that the difference in maximum load between one 20-noded element through thickness and 4 is only just over 2%.

Figure 5: Convergence Study

The material models used are also shown in Figure 4b. An elastic-perfectly plastic rate-independent plasticity material model was used for the limit load analyses, while a multi-linear representation was used for the determination of collapse loads. Both multi-linear kinematic and multilinear isotropic hardening plasticity material models were also used and as expected, proved to have a negligible effect on the collapse load, due to the absence of load cycling. The plasticity algorithm used a von Mises yield criteria with an associative flow rule and modified Newton-Raphson procedure. Both small and large deflection effects were examined.
The finite element model was loaded using a prescribed displacement on the pin, with a contact pair between the pin and the lug shown in Figure 4a. Modelling the pin allowed a more accurate representation of the moment arm, as it included the effect of the pin rolling in the hole due to rotation of the end of the leg. Simple trigonometry showed this error to be of the order of 1%. It was felt that the slight computational overhead of contact was acceptable in return for the avoidance of this error.

4.3 Finite Element Analyses

Three types of finite element analyses were carried out:

- A ***Limit Load*** analysis, as defined in the pressure vessel codes of practice. This type of analysis is often referred to, somewhat misleadingly as it turns out, as a *lower-bound* analysis. Its origin lies in the days of hand calculations and embodies the assumptions of small displacement and an elastic-perfectly plastic material model. It should be noted that a small displacement solution is incapable of simulating the progressive weakening effect of cross-section ovalisation referred to previously. While the loads are applied

- A ***Limit Load with Large Displacement*** analysis. This solution is identical to above, except that large displacement effects are included. The particular nonlinear solution algorithm employed is also capable of handling the reversals of stiffness typical of buckling.
- A ***Plastic Collapse*** analysis, as defined in the pressure vessel codes of practice. This form of analysis uses a multi-linear representation of the material constitutive behaviour, as shown in Figure 4b. The inclusion of strain hardening, as well as large displacement effects, leads to a more faithful representation of reality. In this case, the overhead associated with a multi-linear material model is negligible.

5. Results Comparison

A qualitative comparison of the cross-sectional ovalisation between experiment and FEA is shown in Figure 6a. The finite element deformed mesh corresponds to the end of the test for specimen 7. At this point the bend was sectioned and photographed. No attempt was made to remove the weld metal at the intersection, which clearly had a minimal effect of the results presented here. It is possible however that such weld metal provides some form of reinforcement of the intersection and could for example affect the hot-spot stresses used in fatigue prediction [21]. Clearly the finite element model is capable of reproducing the cross-section ovalisation, which results in a lowering of the bending stiffness of the bend. This ovalisation develops progressively with load, as does the weakening effect. Figure 6b shows the yield front.

Figure 6: Pipe Bend Ovalisation and Yield Front

The summation of the constraint reaction forces for the FEA model, in the direction of the prescribed displacement, was used to determine the collapse and limit load. The resulting load/reaction versus pin displacement, for the Plastic Collapse model, for the mesh with four 20-noded elements through the thickness, is compared with the experimental measurements in Figure 7. It may be observed that the FEA has produced results very close to those of the experiment – a -0.57% variation from the average experimental result. This may appear somewhat fortuitous, given that the percentage variation across the experimental specimens was 3.96%. Interestingly however, this 3.96% variation in results is very close to the 3.53% variation in wall thickness in the experimental specimens reported in Figure 2. This result correlation with thickness is indicative of an almost membrane behaviour across the shell wall. The fact that the convergence studies showed that a single element through the thickness is capable of producing these comparisons, would also tend to support this observation. The thickness of 4mm used in the FEA models is 0.5% above the experimental average, which would notionally result in a decrease of 0.5% in membrane stress levels. The fact that the dimensions used for the FE models are close to the experimental averages for all major bend dimensions, would appear to result in such a favourable comparison. The fact that gross plasticity tends to smooth out the effects of local geometry differences will also improve such comparisons.

Figure 7: Comparison of Experimental and FEA Plastic Collapse Load Deflection Graphs

As shown in Figure 8, large displacement effects are the significant factor. The Limit model has over predicted the strength of the mitre by approximately 43%. The Limit Analysis with large displacement effects is much closer to the Plastic Collapse and experimental results. The reduction in strength due to the cross-section ovalisation is clearly considerable. The effects of a multi-linear material model are also apparent, although much less significant in this case.

Figure 8: Comparison of FEA Plastic Collapse and Limit Load Deflection Graphs

Although not examined in this investigation, when the loading tends to increase the bend angle (opening the bend), the effect of the ovalisation is to increase the second moment of area of the section and therefore progressively stiffen the bend. This in turn results in a substantial increase in the moment required to produce collapse. This is in contrast to the elastic analysis of bends, where there is no difference (apart from a change of sign) between results for moments tending to increase the bend angle and those tending to decrease it. The ovalisation of both smooth and mitred pipe bend cross-sections can act as a strengthening or weakening effect, depending on whether the bend is opening or closing under load. It is the latter that is of greatest concern, although the stiffening associated with opening of the bend could also result in an increase in the terminal reactions at the nozzles of any attached vessels. It is unlikely however that such large displacement effects will be significant in the normal operation of plant.

6. Conclusions

The results presented demonstrate that excellent agreement between experiment and FEA is possible for the plastic collapse of single mitred pipe bends subjected to an in-plane load tending to close the bend angle. These results should therefore provide an excellent benchmark. While 4off 20-noded elements were used through the thickness for comparative purposes, it should be noted that 1 element through the thickness also produced results of reasonable accuracy for the mitres investigated.

The experimental and FEA load-deflection graphs do not show the reversal in stiffness which is characteristic of a buckling failure. It may be concluded therefore that this form of instability does not play a part in failure for this particular problem, with this pipe radius to thickness. It is not always possible to anticipate such instabilities beforehand. In addition it is not always possible to anticipate the significance of weakening mechanisms in structures, such as ovalization, beforehand. It is therefore recommended that where computing resources permit, nonlinear geometrical effects with some form of load-following be used as the default analysis setting.

A so-called lower-bound limit solution to this problem, using an elastic perfectly plastic solution with small displacements, overestimated the maximum load sustained by this component by over 40%. A plastic collapse solution on the other hand, with a multi-linear hardening material model, provided results that were within 1% of the experimental average from the three bends tested. The difference between the results for the multi-linear and the bi-linear elastic-perfectly-plastic models was less than 3%.

References

1. Bore, N et al. A Study of the Educational Development Needs in the Power and Pressure Systems Industry – Interim Report. CCOPPS Project, http://www.ccopps.eu/, Dec. 2007.

2. Wood, J. A Review of Literature for the Structural Assessment of Mitred Pipe Bends. International Journal of Pressure Vessels and Piping, Elsevier Science Ltd., ISSN: 0308-0161. IF-0.830, HL-6.7. Doi: 10.1016/j.ijpvp.2007.11.003. v85, issue 5, May 2008 pp275-294.

3. So, H.S. Single Mitred Pipe Bends Under Bending and Internal Pressure Loads. MSc. Thesis, Victoria Univ of Manchester, March 1971.

4. Kitching, R., Rahimi, G.H. and So, H.S. Plastic Collapse of Single Mitred Pipe Bends. Int. J. Pres. Ves. & Piping, 38, pp129-145, April 1989.

5. Rahimi, G.H. Elastic-Plastic Behaviour of Mitred Pipe Bends. PhD Thesis, University of Manchester, 1991.

6. Robinson, M. and Babaii Kochekseraii, S. Parametric Survey of Upper and Lower Bound Limit In-Plane Bending Moments for Single Mitred Pipe Bends of Various Geometries. Int. J. Pres. Ves. & Piping, v79, pp735-740, 2002.

7. Babaii Kochekseraii, S. Mitred Pipe Bends Subject to Internal Pressure and In-Plane Bending Moment, PhD Thesis, University of Manchester, 1994.

8. Babaii Kochekseraii, S. Finite Element Modelling of Plastic Collapse of Metallic Single Mitred Pipe Bends Subject to In-Plane Bending Moments. Int. J. Pres. Ves. & Piping, v81, pp75-81, 2004.

9. Gresnigt, A.M. Elastic and Plastic Design of Mitred Bends. Proc. 12th Int. Offshore and Polar Engineering Conf., Kitakyushu, Japan, May 26-31, 2002.

10. Gross, N. Report on a Stainless Steel Lobster-Back Duct (Expt. 21). B.W.R.A. Confidential Report FE16/12/51, 1951.

11. Lane, P.H.R. The Design of Fabricated Pipe Bends, Part 1 : Experimental Stress Analysis of a Three-Weld Gusseted Bend. B.W.R.A. Confidential Report FE16/39/56, June 1956.

12. Lane, P.H.R. The Design of Fabricated Pipe Bends and Experimental Stress Analysis of 2-Weld Gusseted Bends. B.W.R.A. Confidential Report FE16/46/57, Dec. 1957.

13. Lane, P.H.R. and Rose, R.T. Experiments on Fabricated Pipe Bends. B.W.R.A. Report No. D5/12/60, 1960.

14. Bond, M.P. A Theoretical and Experimental Investigation of Multi-Mitred Pipe Bends Subjected to Various Types of Loading. PhD Thesis, Victoria Univ of Manchester, Inst. of Sci, & Tech. Feb. 1971.

15. Hose, D.R. Glass reinforced plastic pipework of mixed wall construction. PhD Thesis, University of Manchester, January 1988.

16. Murali, B., Munshi, D., Vaze, K.K. and Kushwaha, H.S. Evaluation of Primary Stress Indices for Mitre Bends and Possibility of Extending to DO/T > 50. Paper F02/4, SMIRT 12, Stuttgart, Aug. 15-20, 1993.

17. American Society of Mechanical Engineers. ASME Boiler and Pressure Vessel Code Section III, Division 1: Rules for Construction of Nuclear Facility Components, Class 1 Components, Subsection NB3600: Piping Design, 1990.

18. B.S.I. Specification for Seamless and Welded Steel Tubes for Automobile, Mechanical and General Engineering Purposes. Part 4: Specific requirements for cold finished seamless steel tubes; BS 6323-4:1982.

19. B.S.I. Tensile Testing of Metallic Materials: Method of Test at Ambient Temperature; BS EN 10002-1:2001.

20. ANSYS 11.0. Ansys Inc,. Canonsburg, PA, USA, 2007, http://www.ansys.com/.

21. Wood, J. Stresses in the Vicinity of an Un-reinforced Mitre Intersection: An Experimental and Finite Element Comparison. Journal of Strain Analysis for Engineering Design, v42, n5, pp325-336, 2007.

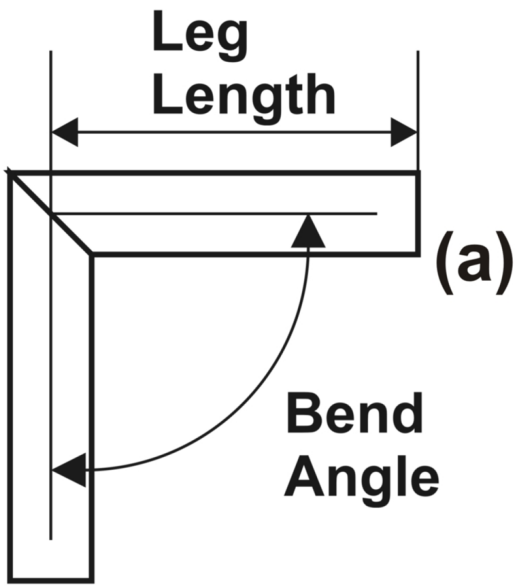

90 Degree Single Segment (2-Weld)

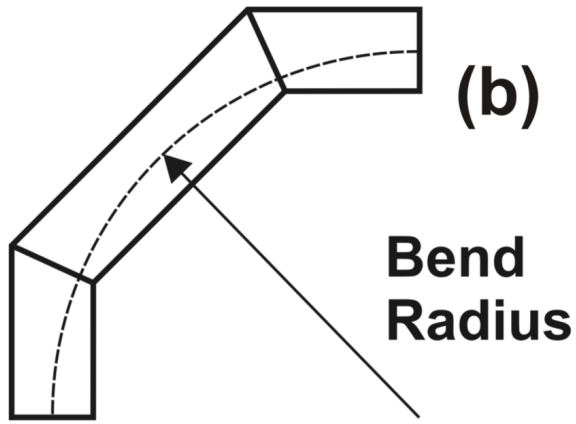

90 Degree Double Segment (3-Weld)

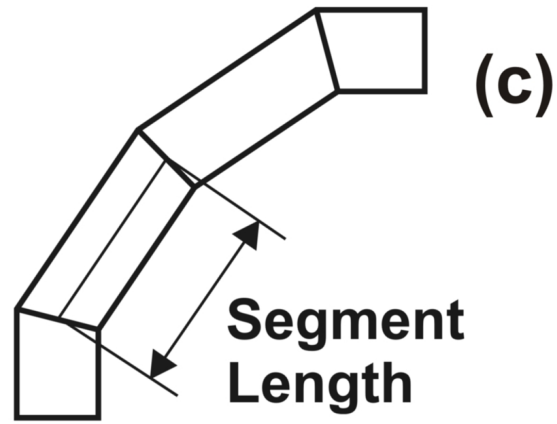

90 Degree Single Mitre

150 Degree Single Mitre

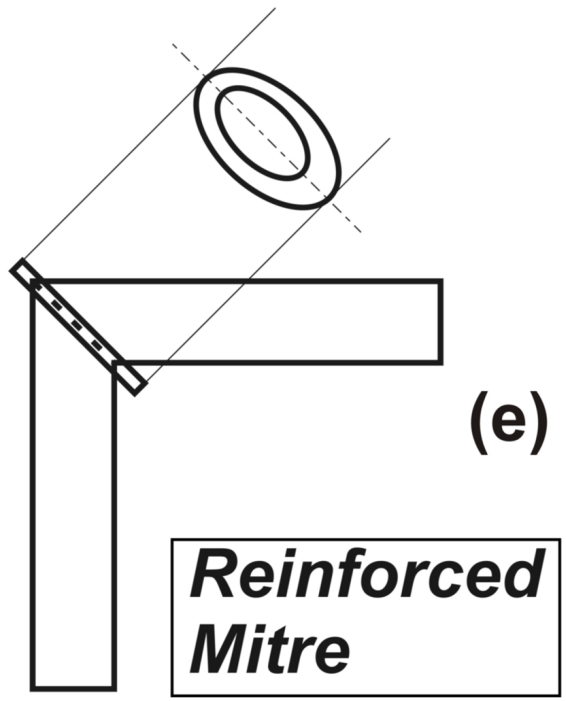

Reinforced Mitre

Fully Fixed Mitre

DIMENSION		SPECIMEN			FE MODEL
		1	*6*	*7*	
A *(deg)*	1	90.045	89.623	89.884	90
L1 *(mm)*	1	497.072	499.010	497.327	502.0
L2 *(mm)*	1	506.506	498.768	500.395	502.0
H1 *(mm)*	1	48.667	52.265	52.057	49.5
H2 *(mm)*	2	47.863	50.537	49.925	49.5
X *(mm)*	2	324.155	318.225	318.921	320
D *(mm)*	3	101.34 - 101.82			100
T *(mm)*	3	3.84 - 4.12			4
W1 *(mm)*	4	60	60	60	60
W2 *(mm)*	4	60	60	60	60
B *(mm)*	4	160	160	160	160
T1 *(mm)*	4	20	20	20	20
T2 *(mm)*	4	20	20	20	20
H3 *(mm)*	4	50	50	50	50
HD *(mm)*	4	20	20	20	20

1 Measured coordinate measurement machine.

2 Derived.

3 Surveyed micrometer.

4 Nominal.

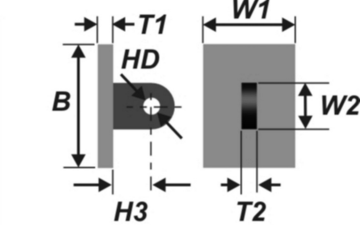

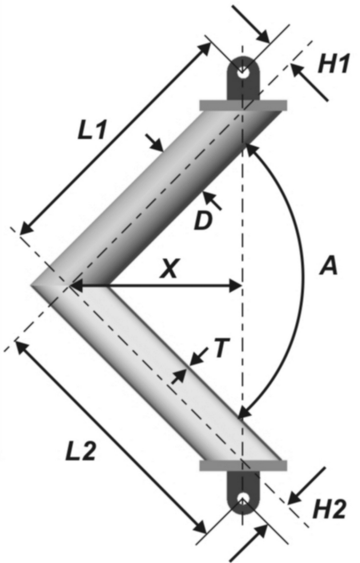

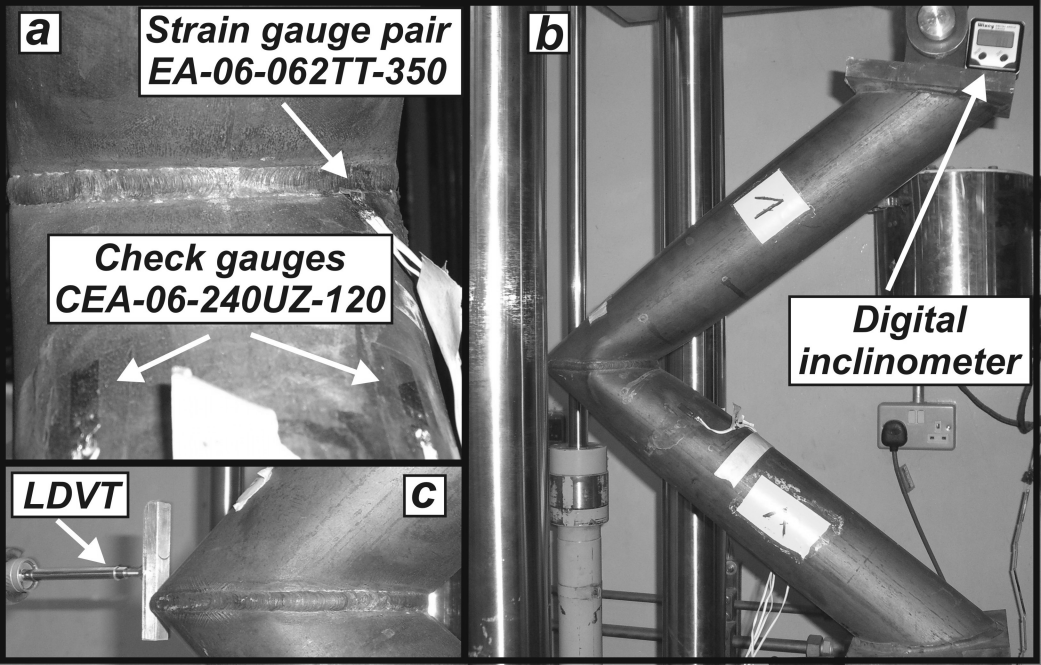
a
Strain gauge pair
EA-06-062TT-350
Check gauges
CEA-06-240UZ-120
LDVT
c
b
Digital
inclinometer

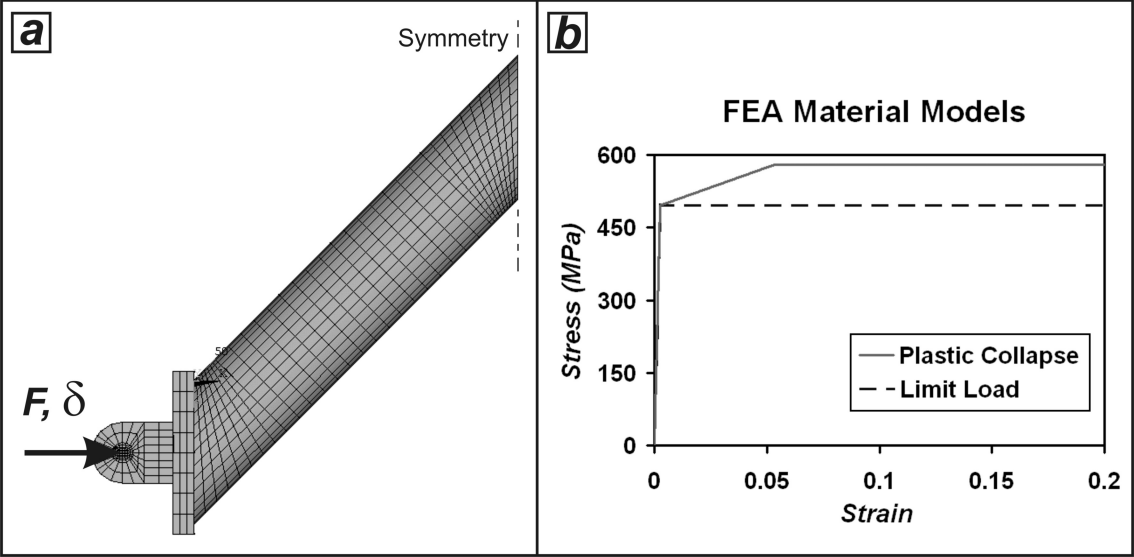
a
Symmetry
F, δ
b
FEA Material Models
600
450
300
150
0
Stress (MPa)
0
0.05
0.1
0.15
0.2
Strain
Plastic Collapse
Limit Load

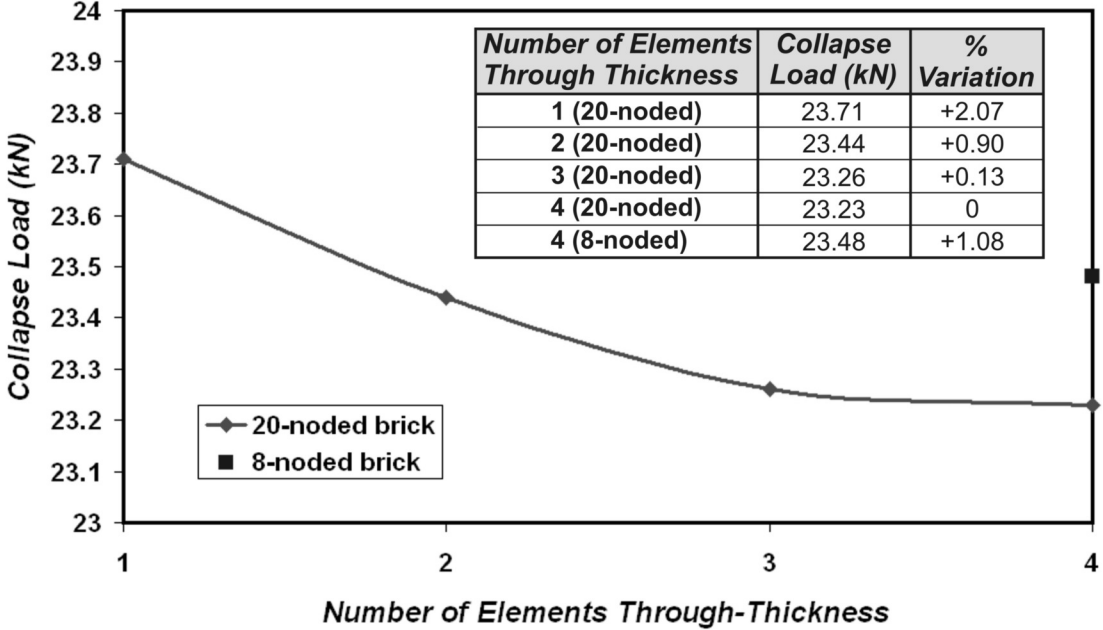

Number of Elements Through Thickness	Collapse Load (kN)	% Variation
1 (20-noded)	23.71	+2.07
2 (20-noded)	23.44	+0.90
3 (20-noded)	23.26	+0.13
4 (20-noded)	23.23	0
4 (8-noded)	23.48	+1.08

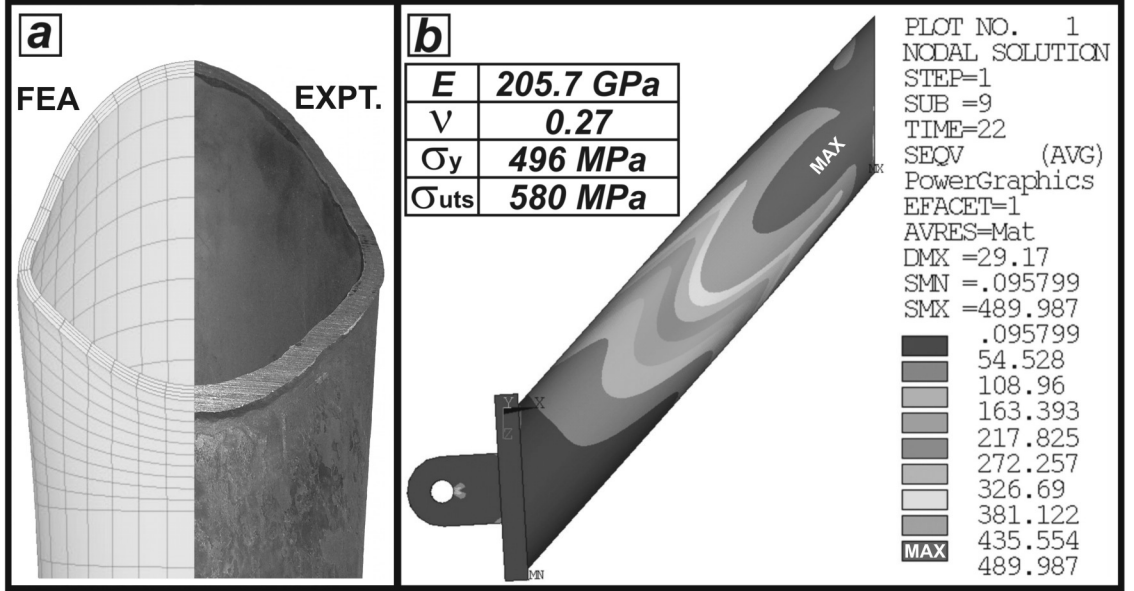
a
FEA
EXPT.
b
E
205.7 GPa
ν
0.27
σy
496 MPa
σuts
580 MPa
MAX
MN
PLOT NO. 1
NODAL SOLUTION
STEP=1
SUB =9
TIME=22
SEQV (AVG)
PowerGraphics
EFACET=1
AVRES=Mat
DMX =29.17
SMN =.095799
SMX =489.987
.095799
54.528
108.96
163.393
217.825
272.257
326.69
381.122
MAX
435.554
489.987

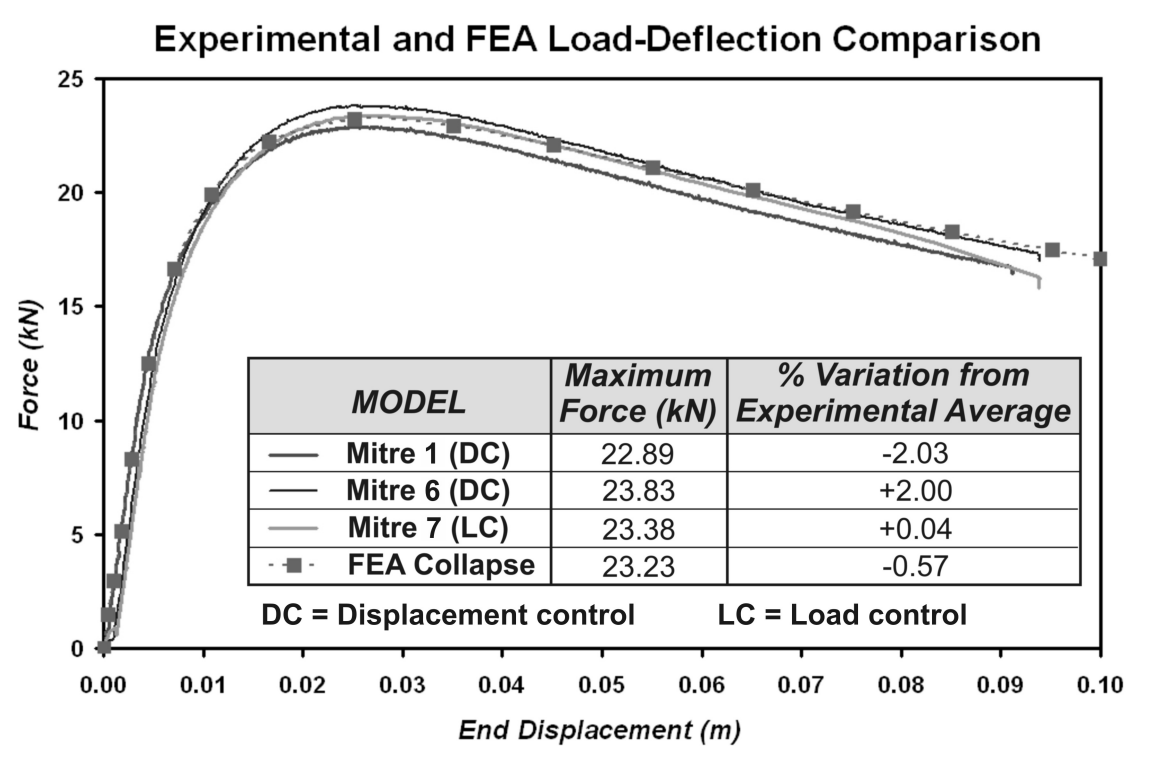
Experimental and FEA Load-Deflection Comparison
Force (kN)
End Displacement (m)
0
5
10
15
20
25
0.00
0.01
0.02
0.03
0.04
0.05
0.06
0.07
0.08
0.09
0.10
MODEL
Maximum Force (kN)
% Variation from Experimental Average
Mitre 1 (DC)
22.89
-2.03
Mitre 6 (DC)
23.83
+2.00
Mitre 7 (LC)
23.38
+0.04
FEA Collapse
23.23
-0.57
DC = Displacement control
LC = Load control

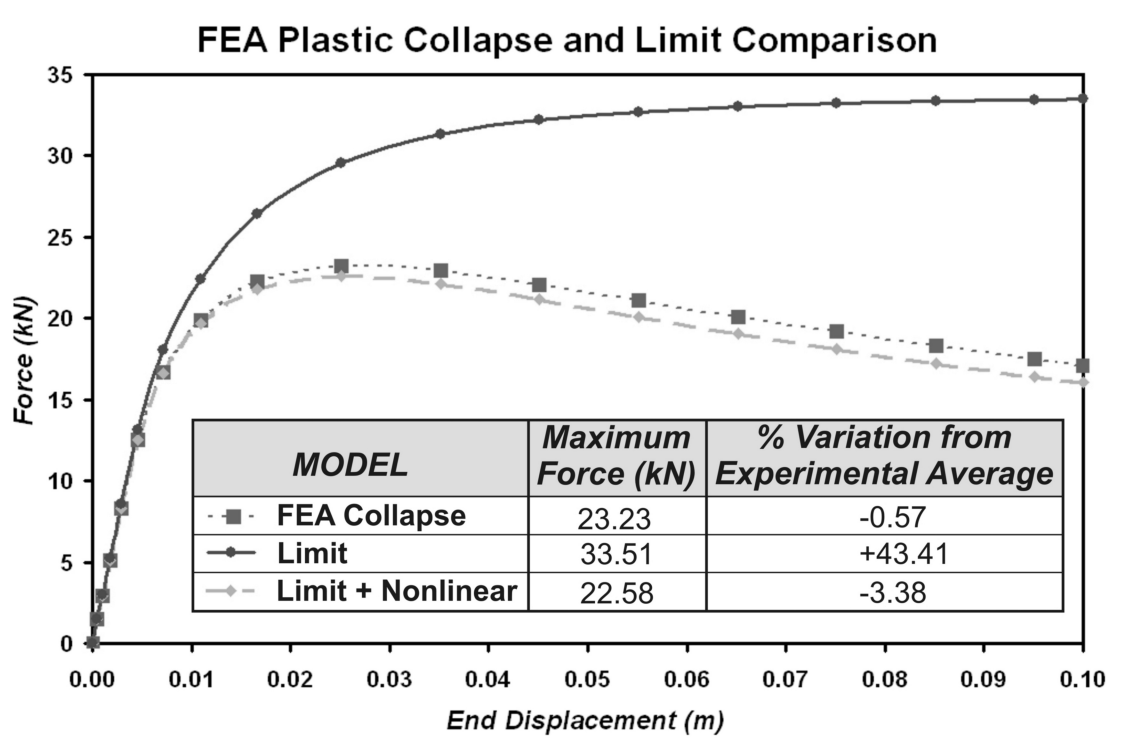
FEA Plastic Collapse and Limit Comparison
Force (kN)
End Displacement (m)
0
5
10
15
20
25
30
35
0.00
0.01
0.02
0.03
0.04
0.05
0.06
0.07
0.08
0.09
0.10
MODEL
Maximum Force (kN)
% Variation from Experimental Average
FEA Collapse
23.23
-0.57
Limit
33.51
+43.41
Limit + Nonlinear
22.58
-3.38